J Mater Sci: Mater Electron (2010) 21:1293–1298
DOI 10.1007/s10854-010-0065-3

Characteristics of ZnS films pulse plated using non-aqueous electrolytes

K. R. Murali · S. Kala · P. Elango

Received: 5 December 2009 / Accepted: 18 January 2010 / Published online: 5 February 2010

Abstract Thin films of ZnS were deposited by the pulse electrodeposition technique employing zinc sulphate and sodium thiosulphate in diethylene glycol solution at 80°C and at different duty cycles in the range 6–50%. The films were polycrystalline exhibiting cubic structure. The intensity of the peaks increased with duty cycle. Transmission measurements indicated interference fringes from which the refractive index fo the films were calculated to be in the range of 2.30–2.70. The band gap of the films was in the range of 3.66–3.62 eV with increase of duty cycle. The films exhibited resistivities in the range of 400–50 ohm cm with increase of duty cycle. The films exhibited higher Photoelectrochemical cell output compared to earlier reports.

1 Introduction

ZnS, a compound semiconductor with a large band-gap energy, has attracted increasing attention due to its application in various optoelectronic devices, such as electroluminescent displays (ELDs) [1, 2], solar cells [3, 4] and light emitting diodes (LEDs) [5]. The preparation methods of ZnS films in these devices are generally magnetron sputtering [6–8], molecular beam epitaxy (MBE) [9], atomic layer epitaxy (ALE) [10], metal–organic chemical vapor deposition (MOCVD) [11], sol–gel [12] and chemical bath deposition (CBD) [13]. Among these methods, magnetron sputtering is a cost effective deposition technique of the film over a large area, which is of great interest for the applications in electroluminescent displays and solar cells. In the most previous reports, ZnS films have been deposited by sputtering from compound targets. Compared to metallic targets, the compound targets are used with slow sputtering rates, and made with high cost. Also, it is well-known that ZnO films can effectively be prepared by reactive magnetron sputtering from a metallic zinc target [14–16]. In particular, the deposition method has its desirable features of high deposition rate, good interfacial adhesion and capability of depositing the film on a large area substrate. Therefore, an alternative preparation method of ZnS films has been proposed, namely sulfurizing the ZnO films deposited by reactive sputtering from a zinc target [17, 18]. RF power has important effects on the properties of the sputter deposited ZnO films, as reported in Refs. [19–21].

In the present work, ZnS films were pulse electrodeposited using nonaqueous solvents for the first time. The structural, optical, electrical and morphological properties are presented and discussed.

2 Experimental methods

Thin ZnS films were deposited by the pulse plating technique at different duty cycles in the range 6–50% employing a current density of 80 $mAcm^{-2}$ on titanium and conducting glass substrates. Deposition at lower duty cycles resulted in thin films (<0.5 μm). Higher duty cycles resulted in large grained films and the film thickness did not increase further. The precursors were 0.1 $MZnSO_4$ and 0.2 M Na2S2O3 in diethylene glycol solution. Higher

K. R. Murali (✉) · S. Kala · P. Elango
Electrochemical Materials Science Division, Central Electrochemical Research Institute, Karaikudi 630 006, India
e-mail: muraliramkrish@gmail.com

S. Kala · P. Elango
Department of Physics, Government Arts College, Coimbatore, India

concentrations of $Na_2S_2O_3$ resulted in preferential deposition of sulphur. The deposition temperature and deposition time were kept constant at 80°C and 30 min, respectively.

Generally in electrodeposition technique for producing a metal or compound, a driving force (i.e., the free energy) in the form of a potential or current is applied to the electrode. Either of these can be used as a variable as in the case of continuous electrodeposition. But modern electronics allows one to make use of these parameters as a function of time. This permits a number of possible ways of varying the conditions.

Four variable parameters are of primary importance in pulse plating. They are:

1. Peak current density, i_p
2. Average current density, i_a
3. ON time and
4. OFF time

The sum of the ON and OFF times constitute one pulse cycle. The duty cycle is defined as follows:

$$\text{Duty cycle} = \frac{\text{ON time}}{\text{ON time} + \text{OFF time}} \times 100\% \quad (1)$$

A duty cycle of 100% corresponds to conventional plating because OFF time is zero.

In practice, pulse plating usually involves a duty cycle of 5% or greater. The average current density (I_a) under pulse plating conditions is defined as

$$\begin{aligned} I_a &= \text{peak current density} \times \text{duty cycle} \\ &= i_p \times \text{duty cycle} \end{aligned} \quad (2)$$

During the ON time the concentration of the metal ions to be deposited is reduced within a certain distance from the cathode surface. This so-called diffusion layer pulsates with the same frequency as the applied pulse current. Its thickness is also related to i_p but reaches a limiting value governed primarily by the diffusion coefficient of the metal ions. During the OFF time the concentration of the metal ions build up again by diffusion from the bulk electrolyte and will reach the equilibrium concentration of the bulk electrolyte if enough time is allowed.

These variables results in two important characteristic features of pulse plating which make it useful for alloy plating as well as property changes as mentioned earlier. They are:

(i) Very high instantaneous current densities and hence very high negative potentials can be reached. The high over potential causes a shift in the ratio of the rates of reactions with different kinetics. This high over potential associated with the high pulse current density greatly influences the nucleation rate because a high energy is available for the formation of new nuclei.

(ii) The second characteristics feature is the influence of the OFF time during which important adsorption and desorption phenomena as well as recrystallization of the deposit occur.

Compared to water, nonaqueous solvents offer an alternative process with some advantages. The proclivity of the chalcogen to exist predominantly in low oxidation states in these baths, and the attendant lack of complications in the electrodeposition chemistry have been the principal motivating factors in the evaluation of nonaqueous media [22].

The films were characterized by X-ray diffraction technique using a PANalytical x-ray diffractometer with Cu Kα radiation. Optical absorption studies were made using a U 3400 UV–vis–NIR Hitachi spectrophotometer. Thickness of the films was measured by Mitutoyo surface profilometer and it was found to be in the range of 0.5–1.0 μm as the duty cycle increased. Surface morphology studies were made by using Molecular Imaging systems Atomic Force Microscope. Photoelectrochemical measurements were made in 1 Mploysulphide (1 M NaOH, 1 M Na_2S, 1M S) electrolyte using a 250 W tungsten halogen lamp.

3 Results and discussion

X-ray diffractograms of films prepared at different duty cycles are shown in Fig. 1. The sample is amorphous at 10% duty cycle. The overall intensity of the reflections increased when the duty cycle increased without the appearance of any new reflections. Thus, no other phases were formed, but only the crystallinity of the formed phase was improved. Above 15% duty cycle, a well-crystallized film was obtained. Phase identification revealed that only cubic ZnS (JCPDS card 77–2100) is formed. Thus, the preparation conditions of a certain technique, not only greatly affects the number of phases formed, but also their microstructural characteristics, such as crystallinity. The crystallite size (D) was measured using Debye–Scherrer's formula [23]

$$D = 0.9\,\lambda/\beta\cos\theta$$

where λ is the wavelength of CuKα radiation and β is the FWHM value. The built in software of the Xpert pro PANalytical XRD system takes care of the instrumental broadening of the XRD peaks and calculates the grain size after correcting for the instrument broadening. Hence the data presented is calculated from the peak width due to the sample alone. The crystallite size increased from 12 to 40 nm as the duty cycle increased from 10 to 50%.

The structural parameters, such as lattice constant and internal stress, were calculated from the XRD data for ZnS

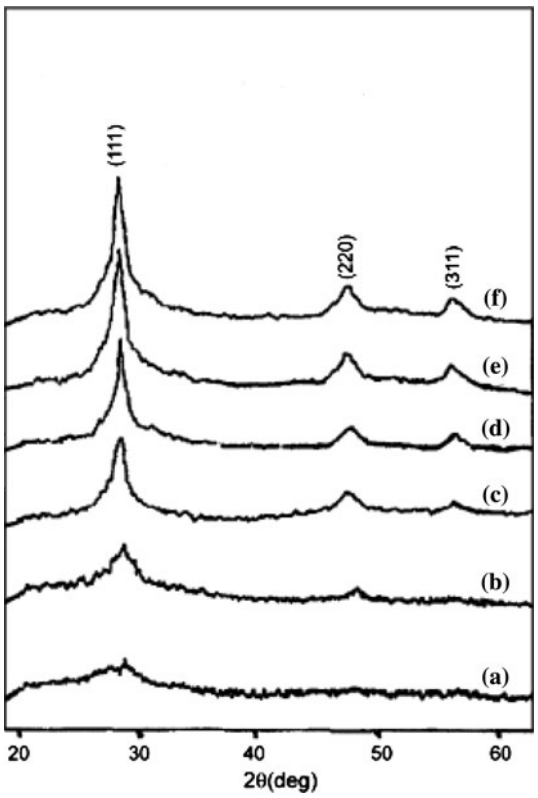

Fig. 1 X-ray diffraction patterns of ZnS films deposited at different duty cycles **a** 6%, **b** 9%, **c** 15%, **d** 25%, **e** 33%, **f** 50%

Table 1 Structural parameters of ZnS films

Duty cycle (%)	Lattice parameters (Å)	Internal stress (GPa)
10	5.35	−0.29
15	5.37	−0.21
30	5.38	−0.14
50	5.40	−0.11

films, and their variation as a function of duty cycle was studied. The lattice parameter a for hexagonal ZnS film was calculated using the relation

$$1/d^2 = 4/3a^2(h^2 + hk + k^2) + l^2/c^2$$

where h, k, l are the lattice planes and d is the inter planar spacing determined using Bragg's equation. The variation of the lattice constant with the duty cycle is presented in Table 1. The lattice constant increased with duty cycle. The change of lattice constant with duty cycle clearly indicated that the crystallites were under stress, leading to either elongation or compression of the lattice constant. This might be due to the change of density and nature of native imperfections with the duty cycle of the film [24]. In general, all polycrystalline thin films are in a state of stress irrespective of their preparation technique. The total stress present in the films is equal to the sum of thermal stress and intrinsic stress in the absence of applied external stress:

$$\sigma_{\text{Total}} = \sigma_{\text{Thermal}} + \sigma_{\text{Intrinsic}}$$

The difference in thermal expansion coefficients of substrate and film gives rise to thermal stress, whereas the difference in lattice constant from that of bulk led to the development of intrinsic stress in the film. In our present study, the thermal stress is calculated using the following relation [25]

$$\sigma_{\text{Thermal}} = (\alpha_{\text{ZnS}} - \alpha_{\text{Titanium}})\,\Delta T\, Y$$

where $\alpha_{\text{ZnS}} = 7.089 \times 10^{-6}/^{\circ}\text{C}$ [26] and $\alpha_{\text{Titanium}} = 8.04 \times 10^{-6}/^{\circ}\text{C}$ are the thermal expansion coefficients of ZnS and titanium, respectively. Y is Young's modulus of ZnS and ΔT is the temperature of the ZnS film during the formation minus the temperature at measurement. The evaluated thermal stress was found to be compressive in nature, and varied in the range of 7–12% of the total stress with the increase of duty cycle. The internal stress in ZnS films was determined using the difference in lattice constants of the film and bulk material using the relation [27]

$$\sigma_{\text{Intrinsic}} = Y(a - a_0)/2\gamma a_0$$

Here, 'a' is the lattice constant measured from the XRD, a_0 is the bulk lattice constant and γ is Poisson's ratio. The variation of internal stress with duty cycle is presented in Table 1.

The transmittance spectra (Fig. 2) were used to calculate the absorption coefficient (α) at different wavelengths using the following relation:

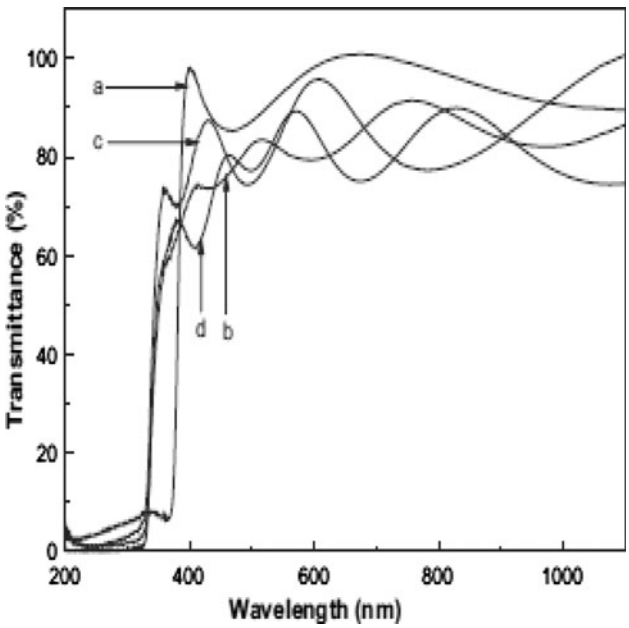

Fig. 2 Optical Transmittance spectra of ZnS films deposited at different duty cycles **a** 50%, **b** 33%, **c** 15%, **d** 9%

$$T = \exp(-\alpha t)$$

where t is the film thickness and T is the transmittance of the film at a particular wavelength. To determined the band gap E_g, we have used Tauc et al.'s plot, where the absorption coefficient α is a parabolic function of the incident energy and optical band gap E_g is given by

$$\alpha = A(h\nu - -E_g)^{\gamma}/h\nu$$

where A is the function of refractive index of the material, reduced mass and speed of light, ν is the transition frequency and the exponent γ characterizes the nature of band transition between the valence band and the conduction band. The band gap can be obtained from extrapolation of the straight-line potion of the $(\alpha h\nu)\gamma$ versus $h\nu$ plot to $\alpha = 0$. A very high value of absorption co-efficient (10^5 cm^{-1}) is observed for all the films. The band gap values have been estimated from the $(\alpha h\nu)^2$ versus $h\nu$ plot, band gap values in the range of 3.66–3.62 eV are obtained as the duty cycle increases. This variation in band gap with duty cycle can be explained by the fact that the grain size increases from 10 to 30 nm as the duty cycle increases. Higher duty cycle obviously leads to an improvement in the crystallinity As the films become homogeneous with increased duty cycle, they tend to acquire higher degree of crystallinity as evident from the sharp edges recorded in the transmission spectra. As the duty cycle increased, the concentration of the structural defects is reduced considerably due to the enlarged crystallite size [28].

The refractive index was calculated using the interference maxima and minima observed at a wavelength from the transmission spectra by the envelope method [29, 30] employing the following equations:

$$n = \left[N + \left(N^2 - n_s^2\right)\right]^2 \quad (1)$$

$$N = \left(n_s^2 + 1\right)/2 + 2n_s(T_{\max} - T_{\min})/T_{\max}\,T_{\min} \quad (2)$$

where, n_s is the refractive index of the substrate, $T_{\max}$ and $T_{\min}$ are the maximum and minimum transmittances at the same wavelength in the fitted envelope curve on a transmittance spectrum. The refractive index value shows a marginal increase from 2.30 to 2.70 with decrease of wavelength. The refractive index value is in good agreement with the reported value [31].

The electrical properties of the ZnS layers were examined at room temperature by resistivity and Hall measurements using Van der Pauw method. Hall measurements were made on the films adopting the procedure reported earlier [32]. For Hall effect measurements, the CdTe layers were transferred from the titanium substrate onto non-conductive epoxy resin by the following method. A sliced vinyl chloride pipe (thickness 3 mm, inner diameter 13 mm, outer diameter 18 mm) was placed on the CdTe deposit on the Au/Cu substrate so that the pipe, or ring, encircled the CdTe-deposited area. Epoxy resin (Torr Seal; Varian Associates) was then poured inside the ring. After the epoxy had coagulated, the back of the substrate was fixed on a tight block with a quick-drying glue and the substrate was stood vertically. Then, the epoxy with the CdTe layer was removed from the substrate by tapping downward on the side of the ring with a mallet, in other words, by applying a shearing force between the CdTe layer and the substrate. In this way, crack-free CdTe layers on the non-conductive substrates could be obtained with high reproducibility. The transferred CdTe layer was cut to a 6 mm square and four gold electrodes with a diameter of 1.5 mm were deposited on each corner by vacuum evaporation through an aluminum foil mask. Gold lead wires with 0.4 mm diameter attached to the gold electrodes with silver paste [33].

The value of the resistivity determined from Van der Pauw method varied from 400 to 50 ohm cm as the duty cycle increased. Hall measurements also indicated the films to exhibit n-type behaviour. The carrier density, mobility and resistivity of the films deposited at different duty cycles are shown in Table 2. The resistivity values are lower than earlier reports [34, 35].

Surface morphology of the films deposited at different duty cycles and transferred to the non conducting epoxy used for electrical measurements is shown in Fig. 3. The grain size is observed to increase from 15 to 35 nm as the duty cycle increases. The RMS value of surface roughness also increases from 2.56 to 4.58 nm as the duty cycle increases.

Photoelectrochemical measurements were made on the films deposited at different duty cycles. The as deposited films exhibited photo activity. Figure 4 shows the load characteristics of the films deposited at different duty cycles. It is observed that the photo-output increases with increase of duty cycle. The PEC output for the electrodes obtained by this technique is higher than those reported earlier [36]. This may due to the fact that the films obtained by this technique possess lower resistivity compared to the earlier reports [36].

Table 2 Transport parameters of ZnS films deposited at different duty cycles

Duty cycle (%)	Resistivity (ohm cm)	Mobility ($cm^2\ v^{-1}\ s^{-1}$)	Carrier density (cm^{-3})
10	400	1.56	1.1×10^{17}
15	300	2.31	0.9×10^{16}
33	170	9.19	0.4×10^{16}
50	50	40.00	0.3×10^{16}

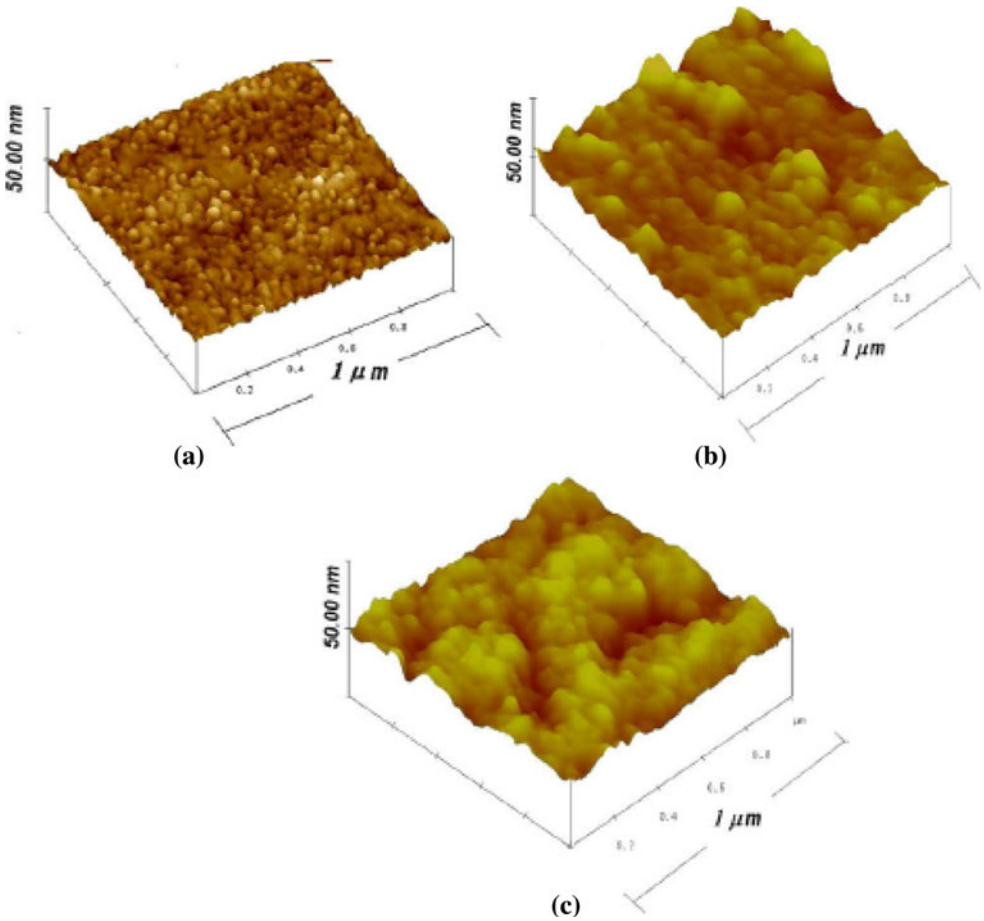

Fig. 3 Atomic force micrographs of ZnS films deposited at different duty cycles **a** 15%, **b** 33%, **c** 50%

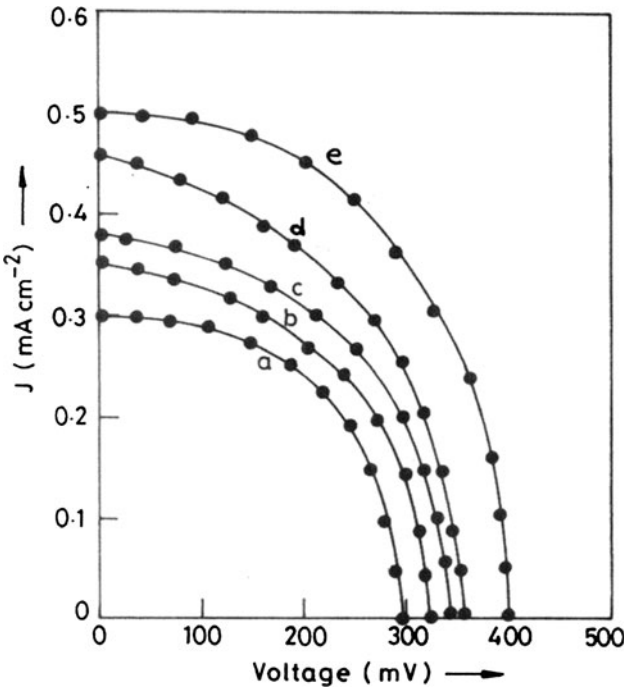

Fig. 4 Current voltage characteristics of ZnS films deposited at different duty cycles **a** 9%, **b** 15%, **c** 25%, **d** 33%, **e** 50%

4 Conclusions

The results of this investigation clearly demonstrate that ZnS films can be easily deposited by the brush plating technique. Films with resistivities in the range of 100–1,000 ohm cm can be obtained. Films with grain size in the range 20–70 nm can be obtained. Photoelectrochemical cells with higher outputs than previous reports can be obtained.

References

1. T. Ogura, A. Mikami, K. Tanaka, K. Taniguchi, M. Yoshida, S. Nakajima, Appl. Phys. Lett. **48**, 1570 (1986)
2. J.S. Lewis, M.R. Davidson, P.H. Holloway, J. Appl. Phys. **92**, 6646 (2002)
3. L.-X. Shao, K.-H. Chang, H.-L. Hwang, Appl. Surf. Sci. **212–213**, 305 (2003)
4. N. Fathy, M. Ichimura, Sol. Energy Mater. Sol. Cells **87**, 747 (2005)
5. H. Katayama, S. Oda, H. Kukimoto, Appl. Phys. Lett. **27**, 697 (1975)
6. H. Xian, P. Benalloul, C. Barthou, J. Benoit, Thin Solid Films **248**, 193 (1994)

7. S.K. Mandal, S. Chaudhuri, A.K. Pal, Thin Solid Films **350**, 209 (1999)
8. A. Nitta, K. Tanaka, Y. Maekawa, M. Kusabiraki, M. Aozasa, Thin Solid Films **384**, 261 (2001)
9. M. Yokoyama, K.-i. Kashiro, S.-i. Ohta, J. Cryst. Growth **81**, 73 (1987)
10. M. Oikkonen, M. Blomberg, T. Tuomi, M. Tammenmaa, Thin Solid Films **124**, 317 (1985)
11. A. Yoshikawa, S. Yamaga, K. Tanaka, H. Kasai, J. Cryst. Growth **72**, 13 (1985)
12. Y. Kavanagh, M.J. Alam, D.C. Cameron, Thin Solid Films **447–448**, 85 (2004)
13. I.O. Oladeji, L. Chow, Thin Solid Films **339**, 148 (1999)
14. G. Xiong, J. Wilkinson, B. Mischuck, S. Tüzemen, K.B. Ucer, R.T. Williams, Appl. Phys. Lett. **80**, 1195 (2002)
15. R. Ondo-Ndong, G. Ferblantier, M. Al Kalfioui, A. Boyer, A. Foucaran, J. Cryst. Growth **255**, 130 (2003)
16. J.J. Chen, Y. Gao, F. Zeng, D.M. Li, F. Pan, Appl. Surf. Sci. **223**, 318 (2004)
17. R. Zhang, B. Wang, D. Wang, L. Wei, Opt. Mater. **27**, 419 (2004)
18. R. Zhang, B. Wang, H. Zhang, L. Wei, Appl. Surf. Sci. **241**, 435 (2005)
19. Y.M. Lu, W.S. Hwang, W.Y. Liu, J.S. Yang, Mater. Chem. Phys. **72**, 269 (2001)
20. X.W. Zhu, Y.Q. Li, Y. Lu, Y.W. Li, Y.B. Xia, Vacuum **81**, 502 (2006)
21. X. Yu, J. Ma, F. Ji, Y. Wang, X. Zhang, C. Cheng, H. Ma, J. Cryst. Growth **274**, 474 (2005)
22. A. Guiner, *Theorie et Technique de la Radiocristallographie* (Editions Dunod, Paris, 1969)
23. X. Dongsheng, G. Guolin, G. Yuguo, Z. Yali, G. Linlin, J. Mater. Chem. **13**, 360 (2003)
24. K. Reichelt, X. Jiang, Thin Solid Films **191**, 91 (1990)
25. K.L. Chopra, *Thin film phenomena* (McGraw Hill, New York, 1969), p. 272
26. V. Kumar, B.S.R. Sastry, Cryst. Res. Tech **36**, 565 (2001)
27. G. Perna, V. Capozzi, M.C. Plantamura, A. Minafra, P.F. Biagi, S. Orlando, V. Marotta, A. Giardini, Appl. Surf. Sci **186**, 521 (2002)
28. G.I. Rusu, M.E. Popa, G.G. Rusu, I. Salaoru, Appl. Surf. Sci **218**, 223 (2003)
29. R. Swanepoel, J. Phys. E **16**, 1214 (1983)
30. J.E. Ramirez-Malo, E. Marquez, P. Villares, R. Jimenez-Garay, Mater. Lett. **17**, 327 (1997)
31. S.M.A. Durrani, A.M. Al-Shukri, A. Iob, E.E. Khawaja, Thin Solid Films **379**, 199 (2000)
32. M. Miyake, K. Murase, T. Hirato, Y. Awakura, J. Electrochem. Soc. **150**, C413 (2003)
33. J.A. Von Windheim, H. Wynands, M. Cocivera, J. Electrochem. Soc. **138**, 3435 (1991)
34. A. Ashour, H.H. Afifi, S.A. Mahmoud, Thin Solid Films **248**, 253 (1994)
35. F. Gode, C. Gumus, M. Zor, J. Cryst. Growth **299**, 136 (2007)
36. N. Fathy, M. Ichimura, Solar Energy Mater Solar Cells **87**, 747 (2005)